International Journal of Obesity (2014) **38,** 1027–1034

www.nature.com/ijo

ORIGINAL ARTICLE

Enhancement of brown fat thermogenesis using chenodeoxycholic acid in mice

JS Teodoro[1,2,5], P Zouhar[3,5], P Flachs[3], K Bardova[3], P Janovska[3], AP Gomes[1,2], FV Duarte[1,2], AT Varela[1,2], AP Rolo[1,4], CM Palmeira[1,2] and J Kopecký[3]

OBJECTIVE: Besides their role in lipid absorption, bile acids (BAs) can act as signalling molecules. Cholic acid was shown to counteract obesity and associated metabolic disorders in high-fat-diet (cHF)-fed mice while enhancing energy expenditure through induction of mitochondrial uncoupling protein 1 (UCP1) and activation of non-shivering thermogenesis in brown adipose tissue (BAT). In this study, the effects of another natural BA, chenodeoxycholic acid (CDCA), on dietary obesity, UCP1 in both interscapular BAT and in white adipose tissue (brite cells in WAT), were characterized in dietary-obese mice.

RESEARCH DESIGN: To induce obesity and associated metabolic disorders, male 2-month-old C57BL/6J mice were fed cHF (35% lipid wt wt^{-1}, mainly corn oil) for 4 months. Mice were then fed either (i) for 8 weeks with cHF or with cHF with two different doses (0.5%, 1%; wt wt^{-1}) of CDCA (8-week reversion); or (ii) for 3 weeks with cHF or with cHF with 1% CDCA, or pair-fed (PF) to match calorie intake of the CDCA mice fed *ad libitum*; mice on standard chow diet were also used (3-week reversion).

RESULTS: In the 8-week reversion, the CDCA intervention resulted in a dose-dependent reduction of obesity, dyslipidaemia and glucose intolerance, which could be largely explained by a transient decrease in food intake. The 3-week reversion revealed mild CDCA-dependent and food intake-independent induction of UCP1-mediated thermogenesis in interscapular BAT, negligible increase of UCP1 in subcutaneous WAT and a shift from carbohydrate to lipid oxidation.

CONCLUSIONS: CDCA could reverse obesity in cHF-fed mice, mainly in response to the reduction in food intake, an effect probably occuring but neglected in previous studies using cholic acid. Nevertheless, CDCA-dependent and food intake-independent induction of UCP1 in BAT (but not in WAT) could contribute to the reduction in adiposity and to the stabilization of the lean phenotype.

International Journal of Obesity (2014) **38,** 1027–1034; doi:10.1038/ijo.2013.230

Keywords: white adipose tissue; uncoupling protein 1; energy expenditure; bile acids

INTRODUCTION

Bile acids (BAs) are essential for lipid absorption in the intestine. More recently, it was discovered that BAs administration could improve several parameters of lipid metabolism.[1] Thus, BAs could beneficially influence the health status of both patients and experimental models (reviewed in Teodoro *et al.*[2]). This finding made BAs a promising new tool for the treatment of metabolic syndrome—that is, the cluster of diseases associated with obesity.

BAs could act as signalling molecules through activation of the farnesoid X receptor (FXR).[3] FXR activation influences glucose and lipid metabolism; namely, it decreases plasma triglyceride (TG) levels by inhibiting lipogenesis and by increasing TG clearance.[3,4] Accordingly, FXR-null mice are obese and hypertriglyceridaemic.[5] FXR is also important for prevention of insulin resistance[6] and hypoglycaemia during fasting,[7] production of hepatic glycogen[8] and differentiation of adipocytes.[9] Moreover, the positive metabolic effect of BAs on glucose control and weight reduction could be mediated by G protein-coupled receptor 5 (TGR5).[10] However, some BAs are not competent activators of TGR5. The most potent natural activator of FXR, chenodeoxycholic acid (CDCA), used as a drug for the treatment of gallstones,[11] has been reported to be both a potent and a not very effective activator of TGR5.[10,12–14] Therefore, the mechanism by which BAs accomplish their beneficial metabolic functions is not yet fully understood.

A new insight into the mechanism of action of BAs was provided by the finding of Watanabe *et al.*[15] that BAs, namely, cholic acid, promote non-shivering thermogenesis in the interscapular brown adipose tissue (BAT) in mice and in skeletal muscle in humans. In BAT, energy expenditure (EE) is mediated by mitochondrial uncoupling protein 1 (UCP1)[16], and induction of the UCP1-based thermogenesis has been proposed as a possible therapeutic strategy against obesity and diabetes.[17,18] The BAs' binding to TGR5 in BAT leads to elevation of cAMP level and consequent activation of thyroid hormone-converting enzyme type 2 iodothyronine deiodinase.[15] BAs therefore facilitate thyroid hormone stimulatory influence on BAT thermogenesis. In fact, treatment with cholic acid was able to reverse diet-induced weight gain.[15] Also, other studies confirmed the ability of BAs to stimulate UCP1-mediated non-shivering thermogenesis in BAT.[10,19,20]

The interest in UCP1-mediated thermogenesis was boosted recently by the discovery of functional BAT in adult humans,[21] as well as by the finding of *Ucp1*-expressing adipocytes,[22–24] which

[1]Center for Neuroscience and Cell Biology, Faculty of Science and Technology, University of Coimbra, Coimbra, Portugal; [2]Department of Life Sciences, Faculty of Science and Technology, University of Coimbra, Coimbra, Portugal; [3]Department of Adipose Tissue Biology, Institute of Physiology Academy of Sciences of the Czech Republic v.v.i., Prague, Czech Republic and [4]Department of Biology, University of Aveiro, Aveiro, Portugal. Correspondence: Dr J Kopecký, Department of Adipose Tissue Biology, Institute of Physiology Academy of Sciences of the Czech Republic v.v.i., Videnska 1083, Prague 14220, Czech Republic.
E-mail: kopecky@biomed.cas.cz
[5]These authors contributed equally to this work.
Received 7 August 2013; revised 11 November 2013; accepted 24 November 2013; accepted article preview online 6 December 2013; advance online publication, 14 January 2014

could be induced in several white adipose tissue (WAT) depots in mice in response to various stimuli and represent a potential target for induction of fat burning (these cells are annotated 'brite' adipocytes in this article, as in Petrovic *et al.*;[25] reviewed in Wu *et al.*[17]). However, whether the brite cells reflect transdifferentiation of white adipocytes[26] or the existence of distinct brown and brite cell lineages (reviewed in Wu *et al.*[17]) is a subject of debate. Similarly, the origin of Ucp1-expressing adipocytes in humans (reviewed in Jespersen *et al.*[27]) and, importantly, the magnitude of energy dissipation in brite cells with respect to that in classical BAT, as well as the contribution of energy dissipation occurring in brite cells to total energy balance (compare Wu *et al.*,[17] and Nedergaard and Cannon[28]), remain all controversial.

We focused here on whether CDCA (similarly to cholic acid; see above) could influence energy balance and reverse the dietary obesity. Our results demonstrated a strong anti-obesity effect of CDCA, which could be explained in large by a transient decrease in food intake. The results suggest that induction of UCP1-mediated thermogenesis in adipocytes in BAT rather than in brite cells could contribute to stabilization of the lean phenotype under these conditions.

MATERIALS AND METHODS

Animals care and diet

C57BL/6J mice were obtained from the Jackson Laboratory (Bar Harbor, ME, USA) and bred at the Institute of Physiology for several generations. Single-caged male mice were maintained at 20 °C on a 12:12-hr light–dark cycle.

Two different experiments were conducted. In the first experiment (8-week reversion), 2-month-old mice were subjected to the high-fat-diet feeding (cHF, lipid content ~35.2% wt wt^{-1}, mainly corn oil, energy density 22.8 kJ g^{-1}; this diet was proven to be obesogenic in C57BL/6J mice, and it contained 15%, 59% and 26% energy as protein, fat and carbohydrate, respectively)[29] for another 4 months to induce obesity and associated metabolic disorders. After that, the animals were randomly divided into three experimental groups ($n = 10$–12 per group) and fed for 8 weeks either the cHF diet, the cHF diet supplemented with 0.5% CDCA (wt wt^{-1}) or the cHF diet supplemented with 1% CDCA (wt wt^{-1}, 95% pure; Sigma-Aldrich, St Louis, MO, USA). All the diets were fed *ad libitum*. Body weight (BW) and food intake were measured every week. During week 6 of the intervention, some of the animals (five mice randomly selected in each group) were subjected to an oral glucose tolerance test (see below). At the end of week 8, all the mice were killed in the morning in fed state by means of cervical dislocation. Plasma was collected (see below), and following tissues were also dissected: liver, gastrocnemius muscle, interscapular BAT, epididymal WAT and subcutaneous WAT (scWAT) from the dorsolumbar region. Moreover, faeces were also collected for further analysis.

In the second experiment (3-week reversion), adult mice already fed the cHF diet for 4 months (see above) were randomly assigned to one of the following: 1) a cHF diet, 2) a cHF diet containing 1% CDCA or 3) a cHF diet with food intake limited to that of animals on 1% CDCA (pair-fed group (PF); $n = 8$ per group). Animals fed standard laboratory chow (STD diet, lipid content ~3.4% wt wt^{-1}, energy density 13.0 kJ g^{-1}; contained 33, 9 and 58% energy as protein, fat and carbohydrate, respectively; extruded Ssniff R/M-H diet, Ssniff Spezialdieten GmbH, Soest, Germany) since weaning at 4 weeks of age were also included in the experiment ($n = 7$). The experiment continued for next 3 weeks. BW and food intake were measured four times each week (see Figures 1c and d). Between day 15 and day 17, indirect calorimetry was performed. At the end of the experiment, mice were killed as described above.

All experiments were performed in accordance with the guidelines for the use and care of laboratory animals of the Institute of Physiology, the directive of the European Communities Council (2010/63/EU) and the Principles of Laboratory Animal Care (NIH publication no. 85–23, revised 1985).

Evaluation of plasma parameters, glucose homeostasis and TG content in tissues and faeces

Blood was collected and analysed as described previously;[30] glycaemia, plasma levels of non-esterified fatty acids, TG, cholesterol, insulin and multimeric forms of adiponectin were evaluated. The remaining plasma was frozen at −80 °C for measurement of the activity of liver enzymes, as previously described.[31] Oral glucose tolerance test was conducted as described in Medrikova *et al.*[30] TG content in tissues and faeces was assessed.[32]

Light microscopy and immunohistology analysis

Adipose tissue samples were fixed in 10% neutral buffered formalin (Sigma-Aldrich) and embedded in paraffin. Sections (5 μm) were stained with haematoxylin–eosin for morphometry, or processed to detect UCP1-positive cells, using a rabbit anti-hamster UCP1 antibody.[33] Sections were deparaffinized and rehydrated, and 10 mM sodium citrate (pH 6.0) was used for antigen retrieval. Immunohistological detection of UCP1 was performed as follows: a) incubation with 3% hydrogen peroxide in methanol at room temperature for 10 min; b) incubation with the diluted goat serum 1:50 at room temperature for 30 min; c) incubation with the primary antibody diluted 1:4000 at 4 °C overnight; d) incubation with the secondary antibody anti-rabbit IgG biotinylated (Vector laboratories, Burlingame, CA, USA) 1:200 at room temperature for 1 h; e) incubation with ABC (Vectastain ABC kit, Vector laboratories) at room temperature for 1 h; f) visualization using diaminobenzidine. For each treatment, a negative control without the primary antibody was used. BAT was used as a positive control for UCP1 immunoreactivity. Digital images were captured using an Olympus AX70 light microscope and a DP 70 camera (Olympus, Tokyo, Japan). Morphometric analysis was performed using Imaging Software NIS-Elements AR3.0 (Laboratory Imaging, Prague, Czech Republic). The morphometry data are based on measurements of ~800 cells taken randomly from two to three different sections per animal (see Medrikova *et al.*[30]).

RNA isolation and real-time PCR

Total RNA was isolated from flash-frozen tissue (kit from Qiagen GmbH, Hilden, Germany). RNA yields were quantified using a Nanodrop instrument (Thermo Scientific, Waltham, MA, USA). Complementary DNA was produced using 1 μg of RNA with a Bio-Rad iScript cDNA synthesis kit (Bio-Rad, Hercules, CA, USA). Gene expression was evaluated using real-time PCR, LightCycler (Roche Diagnostics, Mannheim, Germany) and MiniOpticon (Bio-Rad) equipments. Primers used and their sequences are described in Supplementary Table S1.

Quantification of UCP1 using Western blots

Tissue membranous fraction was prepared using 70 mg interscapular BAT or 100 mg scWAT samples, by homogenization in a buffer containing 250 mM sucrose, 50 mM Tris, 5 mM Na-EDTA, 174 μg ml^{-1} phenylmethanesulphonylfluoride, 1 μg ml^{-1} aprotinin, leupeptin and pepstatin, followed by centrifugation at 100 000 *g*, for 45 min, at 4 °C. Membranous sample aliquots (2–5 μg protein) were then analysed using western blots and 10% polyacrylamide gels.[33] Immunodetection of UCP1 was performed similarly to the detection of adiponectin multimeric forms in plasma,[30] except that anti-UCP1 antibody (1:500)[33] and a secondary infrared dye-conjugated antibody (1:5000) were used. Mitochondria isolated from interscapular BAT of adult C57BL/6J mice reared at 4 °C were used to quantify the relative UCP1 content in each sample (the detection limit for UCP1 was about 0.5 μg of BAT mitochondrial protein and relative UCP1 content in whole interscapular BAT was also calculated. Protein was measured using bicinchoninic acid.[34]

Indirect calorimetry

To evaluate EE and fuel partitioning, indirect calorimetry was performed using INCA system from Somedic (Horby, Sweden).[35,36] Briefly, the measurements were performed in individually caged mice (Eurostandard type II mouse plastic cages; ~6000 ml; Techniplast, Milan, Italy), with the cages placed in a sealed measuring chamber equipped with thermostatically controlled heat exchangers at 22 °C. Oxygen consumption (VO_2) and carbon dioxide production (VCO_2) were recorded every 2 min under a constant airflow rate (1000 ml min^{-1}) for 24 h, starting at 0800 hours. EE was calculated using the following equation: $EE\ (cal) = 3.9 \times VO_2\ (ml) + 1.1 \times VCO_2\ (ml)$.[37,38] The level of substrate partitioning was estimated by calculating respiratory quotient (RQ; that is, VCO_2/VO_2 ratio). To compare subtle differences between groups, the percent relative cumulative frequency (PRCF) curves were constructed on the basis of RQ values pooled from all the animals within a given dietary group ($n = 7$–8) during the whole measurement

period, as described before.[35] Provided that the PRCF curves represent the normally distributed data, the values of 50th percentile of PRCF (EC_{50}) based on each individual animal correspond to RQ values.

Statistical analysis

All values are reported as means ± s.e.m. Statistical significance was analysed as indicated by one-way ANOVA with a Holm–Sidac correction in SigmaPlot 10 software (Systat Software, Point Richmond, CA, USA). The PRCF curves were analysed using nonlinear regression using SigmaPlot. Differences in EE were evaluated by ANCOVA using NCSS software. Differences were considered significant when $P<0.05$.

RESULTS

Reversal of dietary obesity and associated disorders in response to CDCA

First, the effects of CDCA admixed to the cHF diet (0.5% and 1% CDCA) were examined in the 8-week reversion of dietary obesity. Immediately following the switch to the CDCA-containing diets, food intake rapidly decreased reflecting the dose of CDCA, and it returned to the level observed in the control cHF-fed mice within 2–3 weeks of the intervention (Figure 1a). This transient drop due to habituation of mice to the new diets was not accompanied by any changes in plasma levels of liver transaminases (Table 1), arguing against hepatotoxic effects of CDCA. The transient decrease in food intake coincided with a CDCA dose-dependent decrease in BW (Figure 1b), with a maximum reduction reached by the end of week 2 of the intervention. Surprisingly, in spite of the normalization of food intake in the CDCA-intervention groups following week 2, the depression of BW lasted stable till the end of the experiment at week 8 (Figure 1b).

At week 8, plasma lipid levels (namely, TG and cholesterol) were decreased by the CDCA interventions, with a dose-dependent effect on TG levels, and maximum effect on cholesterol levels observed already at the lower CDCA dose (Table 1). Dose-dependent lowering of glycaemia, insulinaemia and glucose intolerance (manifested by changes of area under curve in glucose tolerance test) in response to CDCA documented improvement of glucose homeostasis by the interventions, which was in accordance with the increase in the ratio of high molecular weight adiponectin/total adiponectin plasma levels (Table 1). Lipid (TG and cholesterol) content in faeces was slightly decreased by CDCA treatment, independently of the dose.

Changes in BW could be explained by the changes in adiposity, as documented by weights of both epididymal WAT and scWAT (Table 1). Furthermore, the CDCA intervention prevented ectopic TG accumulation in liver and muscle (Table 1). Thus, the 8-week reversion experiment revealed strong normalization of BW and obesity-associated phenotypes in response to the CDCA intervention. However, it remained to be established what was the contribution of the transient decrease in food intake to the lasting effects of the intervention.

Reduction of adiposity in response to CDCA in a pair-feeding experiment

To dissect the role of the transient decrease in food intake and the CDCA-induced metabolic effects in the anti-obesity effect of the drug, the 3-week reversion experiment was conducted (Figures 1c and d), in which PF animals were also included. The duration of intervention was shortened to 3 weeks, in order to focus on the period when the decline in food intake occurred (see above). The transient decrease in food intake in the CDCA mice, normalized within 3 weeks (Figure 1c), was associated with a drop in BW, almost to the level of mice fed the STD diet since weaning (Figure 1d). This drop could be explained by the decrease in food intake, as it was also observed in the PF mice (Figure 1d). The animals maintained the decreased BW even after reaching the normal food consumption (Figures 1c and d).

Adipose tissue in the 3-week reversion experiment

Dietary obesity was associated with a strong increase in adiposity, as indicated by the differences in weights of all fat depots analysed in the STD mice and the cHF mice (Table 2). Weights of epididymal WAT and scWAT depots, as well as interscapular BAT, were significantly decreased in the PF mice (Table 2).

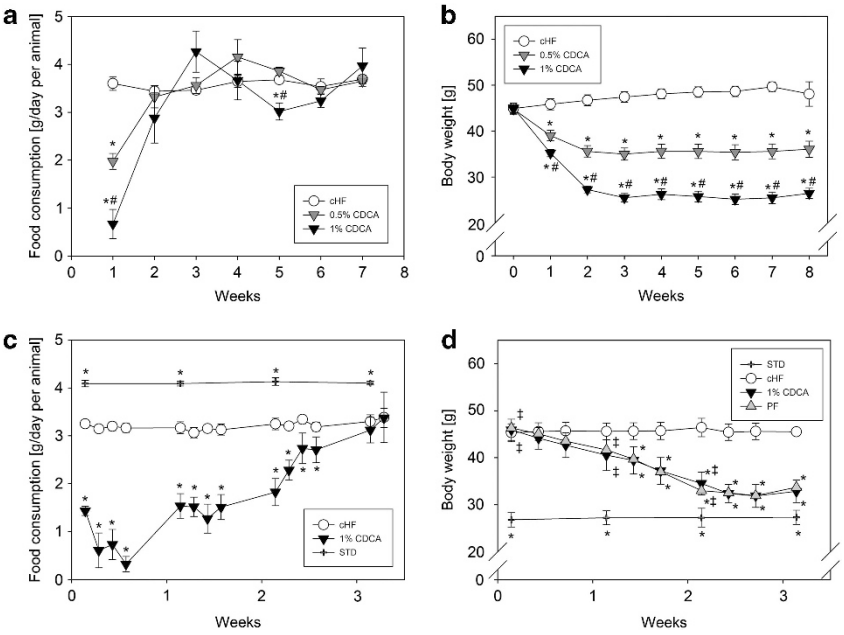

Figure 1. Growth curves and food intake. (**a**, **b**) Food intake (**a**) and growth curve (**b**) during the 8-week reversion experiment ($n=10$–12); (**c**, **d**) food intake (**c**) and growth curve (**d**) during the 3-week reversion experiment ($n=8$, except for STD, where $n=4$). Data are means ± s.e.m. *Significantly different in comparison to the cHF group; #significantly different in comparison to the 0.5% CDCA group (only in **a** and **b**); ‡significantly different in comparison to the STD group (only in **d**). cHF, high-fat diet; 0.5 and 1% CDCA, high-fat diet supplemented with 0.5% and 1% CDCA, respectively; PF, pair-fed group; STD, standard chow diet.

Table 1. Parameters measured in plasma, tissues and faeces at the end of the 8-week reversion experiment

	cHF	*0.5% CDCA*	*1% CDCA*
Plasma levels			
TG (mmol l^{-1})	1.56 ± 0.12	1.08 ± 0.12[a]	0.83 ± 0.10[a]
NEFA (mmol l^{-1})	0.86 ± 0.04	0.85 ± 0.04	0.65 ± 0.04[a,b]
Cholesterol (mmol l^{-1})	5.27 ± 0.26	3.15 ± 0.26[a]	2.70 ± 0.42[a]
Glucose (mg dl^{-1})	257 ± 10	191 ± 13[a]	143 ± 19[a]
Insulin (ng ml^{-1})	4.53 ± 0.43	0.71 ± 0.10[a]	0.19 ± 0.03[a]
Adiponectin HMW (AU)	0.43 ± 0.03	0.47 ± 0.04	0.62 ± 0.07[a]
Total (AU)	1.02 ± 0.06	0.98 ± 0.07	1.20 ± 0.10
HMW/totals	0.42 ± 0.02	0.48 ± 0.03	0.51 ± 0.03
Aspartate transaminase (uCAT l^{-1})	3.02 ± 0.32	3.01 ± 0.39	3.26 ± 0.30
Alanine transaminase (uCAT l^{-1})	1.12 ± 0.16	0.62 ± 0.03	0.88 ± 0.08
Oral glucose tolerance test			
Total AUC (mmol l^{-1} Glc 180 min)	3042 ± 189	2524 ± 158[a]	1654 ± 82[a,b]
Weight of tissues			
eWAT (mg)	2241 ± 105	1419 ± 147[a]	513 ± 66[a,b]
scWAT (mg)	1295 ± 60	612 ± 102[a]	191 ± 19[a,b]
Liver (mg)	2328 ± 132	1873 ± 95	2060 ± 204
Tissue TG content			
Liver TG (mg g^{-1} tissue)	377 ± 41	49 ± 6[a]	30 ± 1[a,b]
Muscle TG (mg g^{-1} tissue)	113 ± 11	50 ± 7[a]	35 ± 7[a]
Faeces lipid content			
TG (mg g^{-1})	62.8 ± 14	47.5 ± 4.7	49.2 ± 2.9
Cholesterol (mg g^{-1})	12.3 ± 0.8	10.4 ± 0.4[a]	10.5 ± 0.3[a]

Abbreviations: AUC, area under the curve; CDCA, chenodeoxycholic acid; cHF, high-fat diet; eWAT, epididymal WAT; HMW, high molecular weight; NEFA, non-esterified fatty acid; scWAT, subcutaneous WAT; TG, plasma triglyceride. Data are means ± s.e.m. ($n = 10$–12, except for oral glucose tolerance test, where $n = 5$; see Materials and Methods). [a]Significant differences in comparison to the cHF group. [b]Significant differences in comparison to the 0.5% CDCA group.

Table 2. Fat depots at the end of the 3-week reversion experiment

	STD	*cHF*	*1% CDCA*	*PF*
Weight of tissues				
eWAT (mg)	553 ± 94[a]	2490 ± 208	899 ± 147[a]	979 ± 154[a]
scWAT (mg)	183 ± 14[a]	1163 ± 168	417 ± 78[a]	498 ± 83[a]
Interscapular BAT (mg)	121 ± 19[a]	228 ± 20	92 ± 9[a]	125 ± 17[a]
Average adipocyte area				
scWAT (μm^2)	1040 ± 190[a]	3474 ± 240	1652 ± 193[a]	2191 ± 186[a,b]

Abbreviations: BAT, brown adipose tissue; CDCA, chenodeoxycholic acid; cHF, high-fat diet; eWAT, epididymal WAT; PF, pair-fed group; scWAT, subcutaneous WAT; STD, standard chow diet. Data are shown as means ± s.e.m. ($n = 8$, except for STD, where $n = 4$; see Materials and Methods). [a]Significant differences in comparison to the cHF group. [b]Significant differences in comparison to the STD group.

Morphometry of adipocytes in scWAT indicated that the differences in adiposity were reflected by the size of adipocytes (Table 2). A similar conclusion could be made by a simple inspection of histological sections from both interscapular BAT (Figure 2a) and scWAT (Figure 3a). Weights of all fat depots analysed, as well as the size of adipocytes in scWAT, tended to be smaller in the CDCA as compared with the PF mice, but the differences were not statistically significant (Table 2).

To learn whether the reduction in BW and adiposity in response to both PF and CDCA intervention could be explained by induction of UCP1-mediated thermogenesis, as previously observed in the case of cholic acid,[15] *Ucp1* gene transcript levels in the interscapular BAT were quantified. As compared with the cHF mice, *Ucp1* gene expression was highly induced in the CDCA mice (Figure 2b), which was also in accordance with the increased expression of the *Prdm16* gene (which is essential for *Ucp1* gene expression and for the activation of the UCP1-mediated thermogenesis[39]) as well as the induction of selected markers of mitochondrial biogenesis (such as *Ppargc1a*, *Slc25a4* and *Cox4i1*; Figure 2b). On the other hand, no induction of these genes could be observed in the PF mice (Figure 2b). Total thermogenic activity of interscapular BAT could be assessed by evaluation of UCP1 content per depot.[28] Therefore, UCP1 was quantified in the membranous fraction prepared from interscapular BAT using western blots (data not shown). Although total UCP1 content was similar in the STD, cHF and PF mice, it was significantly increased in response to the CDCA intervention, and it was ~1.5-fold higher in the CDCA as compared with the cHF mice (Figure 2c).

Also in scWAT of the CDCA and PF mice, *Ucp1* gene transcript was detected. No *Ucp1* gene transcript could be detected in the cHF mice, and the transcript levels were much higher in the CDCA as compared with the PF mice. However, even in the CDCA mice, *Ucp1* transcript levels in scWAT were at least three orders of magnitude lower as compared with those in interscapular BAT of these mice (compare *Y* axes in Figures 2b and 3b, where *Ucp1* transcript levels were estimated under identical conditions).

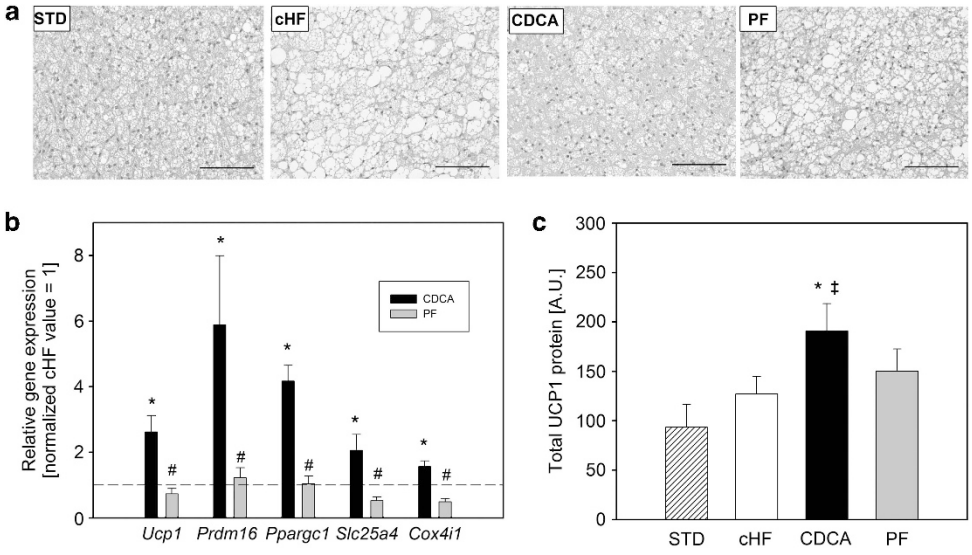

Figure 2. Interscapular BAT parameters in the 3-week reversion experiment. (**a**) Representative images of BAT. (**b**) Relative gene expression (cHF = 1, dashed line); data were normalized using 18S RNA as a housekeeping gene. (**c**) Content of UCP1 protein in whole interscapular BAT. *Significantly different in comparison to the cHF group; #significantly different in comparison to the CDCA group; ‡significantly different in comparison to the STD group. Data are means ± s.e.m. ($n = 8$, except for STD, where $n = 4$). (**a**) Bar = 0.1 mm. CDCA, high-fat diet supplemented with 1% CDCA; cHF, high-fat diet; PF, pair-fed group; STD, standard chow diet.

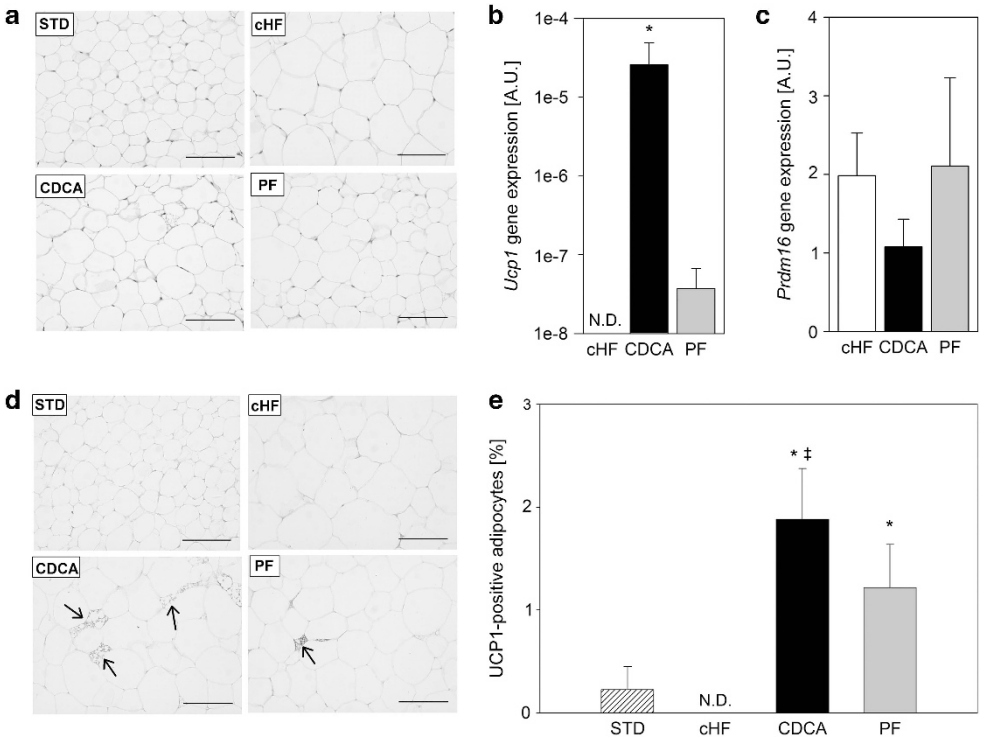

Figure 3. scWAT parameters in the 3-week reversion experiment. (**a**) Representative images of WAT. (**b** and **c**) *Ucp1* and *Prdm16* gene expression; data were normalized using 18S RNA as a housekeeping gene. (**d**) Representative images of immunostaining for UCP1; UCP1-positive cells are indicated by arrows. (**e**) Graphical representation of the percentage of UCP1-positive cells relative to all adipocytes visualized. *Significantly different in comparison to the cHF group; ‡significantly different in comparison to the STD group. Data are means ± s.e.m. ($n = 8$, except for STD, where $n = 4$). (**a** and **d**) Bar = 0.1 mm. CDCA, high-fat diet supplemented with 1% CDCA; cHF, high-fat diet; ND, not detected; PF, pair-fed group; STD, standard chow diet.

However, unlike in BAT, in scWAT, *Prdm16* gene expression did not reflect the activity of *Ucp1* gene, and expression of *Prdm16* gene in the cHF, CDCA and PF mice was similar (Figure 3c). In contrast to BAT, even in scWAT of the CDCA mice, we could not detect any UCP1 using western blots, indicating that in spite of the stimulation of *Ucp1* gene expression in WAT, UCP1 levels in this tissue were relatively low and that they were under the detection limit of the method (data not shown). Immunohistological analysis

revealed some UCP1-positive adipocytes (that is, 'brite' cells) in scWAT, especially in the CDCA mice (Figures 3d and e), but not in eWAT (data not shown).

Indirect calorimetry in the 3-week reversion experiment

To evaluate the effects of the CDCA intervention on EE and fuel partitioning, indirect calorimetry was performed during the third week of the 3-week reversion experiment. As expected, in all the groups, that is, the cHF, CDCA and PF mice, EE was relatively high during the dark phase of the day, when the mice are known to be active. However, except for a decline in EE during the dark phase in the PF mice, the expected effect of a limited food supply in the PF mice, no major differences in the time course of EE between the groups were observed (Figure 4a). Accordingly, analysis of mean EE over the whole day has not revealed any significant differences between the groups when the values are expressed per the whole animal even when evaluated by ANCOVA reflecting BW (Figure 4d). However, when EE was adjusted to BW, both the CDCA mice and the PF mice exhibited higher EE as compared with the control mice fed the cHF diet (Figure 4e). Whether this could suggest CDCA-induced increase in EE is a matter of debate (see Discussion). The evaluation of RQ, the marker of fuel partitioning, during the day revealed a decline in RQ during the dark phase in the PF mice (Figure 4b), suggesting a gradual shift from carbohydrate to lipid oxidation in response to the limited food supply (see above). Moreover, during the dark but not during the light phase of the day, the CDCA mice exhibited a lower RQ as compared with the cHF mice (Figure 4b). The robust PRCF analysis of the RQ data, which takes into account all the RQ values measured in each group (see Materials and methods), supported the shift from carbohydrate to lipid oxidation in response to pair-feeding, and, importantly, it also suggested a food consumption-independent shift to lipid oxidation in response to the CDCA intervention (Figure 4c). The PRCF data were evaluated for the whole day rather than separately for the light and the dark phase of day, to eliminate the influence of the shift in rhythmicity elicited in response to the pair-feeding. Also, the mean RQ during the whole day (Figure 4f) as well as the 50th percentile of the PRCF data (Figure 4g) tended to be the lowest in the CDCA mice, but these differences were not statistically significant. Taken together, these data suggest that CDCA increased lipid oxidation in expense of carbohydrate oxidation, especially during the dark phase of the day, independent of food intake.

DISCUSSION

In accordance with the previous studies using cholic acid in cHF-fed mice performed by the group of Auwerx,[10,15,20] we have demonstrated that supplementation of a cHF using BAs, namely CDCA, could reverse dietary obesity and associated metabolic disorders. Thus, in response to the 8-week intervention, a dose-dependent effect of CDCA was observed with respect to the reduction of obesity, amelioration of dyslipidaemia, normalization of glucose homeostasis and reduction of ectopic accumulation of lipids in the liver and skeletal muscle. No detrimental effects on hepatic markers were observed, and in accordance with the effect of cholic acid[15] used in several of the previous studies,[10,15,20] the CDCA intervention had no effect on lipid absorption.

Most of the above mentioned beneficial metabolic effects of CDCA could be related to a transient decrease in food consumption observed at the beginning of the intervention. This is not consistent with the outcomes of the previous studies in mice,[10,15,20] in which admixing of cholic acid to cHF was

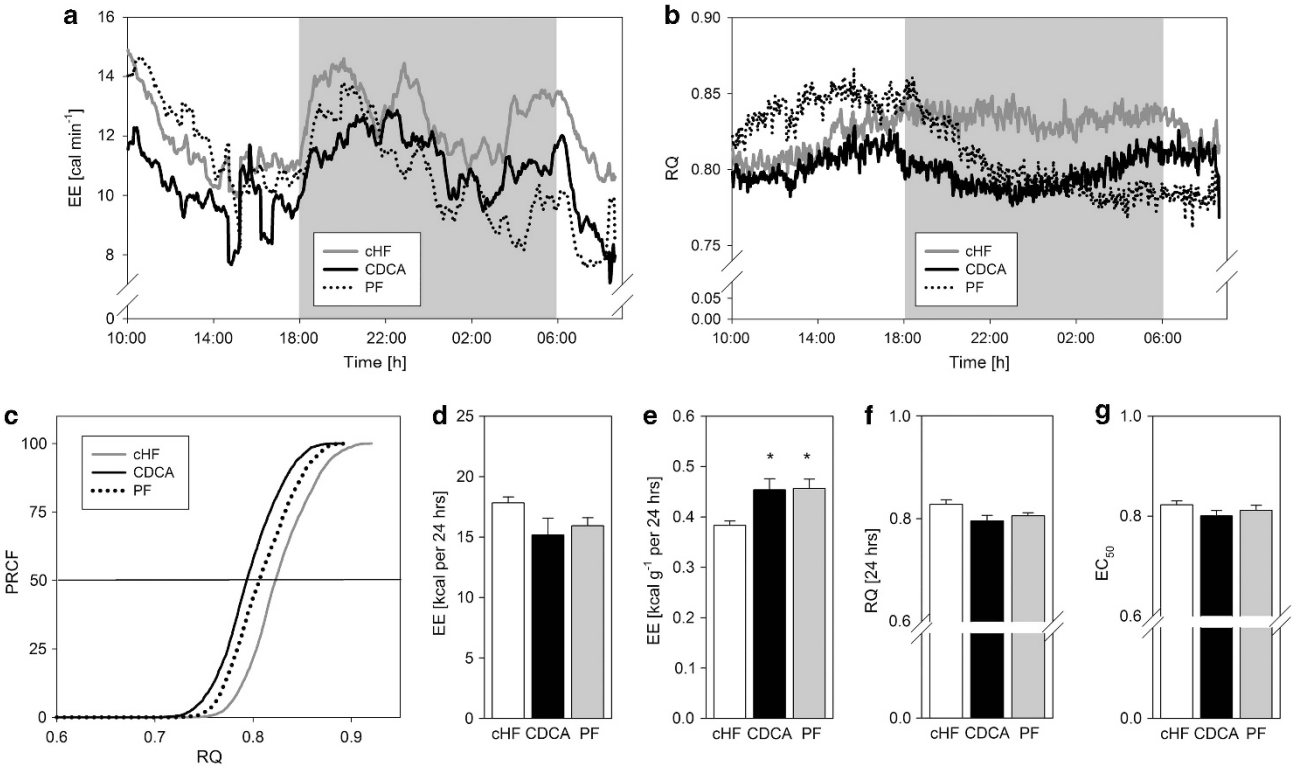

Figure 4. Indirect calorimetry performed between day 15 and day 17 of the 3-week reversion experiment. (**a**) Time course of the measurements of EE. (**b**) Time course of the RQ measurements; grey area in **a** and **b** represents the dark phase of the day. (**c**) Plot of PRCF of RQ values during the whole 24-h measurement period; each curve represents data pooled from all mice within a given group ($n = 7$–8; ~5 000 RQ measurements per curve). (**d**) Total EE per mouse (24 h). (**e**) Total EE per g BW (24 h). (**f**) Mean RQ (24 h). (**g**) 50th percentile value of PRCF (EC_{50}) derived from (**c**). *Significantly different in comparison to the cHF group. CDCA, high-fat diet supplemented with 1% CDCA; cHF, high-fat diet; PF, pair-fed group.

interpreted not to affect food consumption. However, in these previous studies, food intake was adjusted to BW of the animals (see Figure 1f in Watanabe *et al.*,[15] Figure 1a of Watanabe *et al.*,[20] Figure 1a of Watanabe *et al.*[10]), whereas in our study, food intake per mouse was considered. Therefore, in the previous studies, the decrease in absolute food intake could be masked when adjusted to BW, as BW was decreased in response to the cholic acid intervention. Owing to a relatively low specific metabolic rate of WAT, it is conceivable that non-adjusted (or lean body mass-adjusted) rather than total body mass-adjusted food intake should be considered when judging the impact of food intake on obesity.[40–42] However, neither lean body mass nor fat-free mass was evaluated in this study.

Therefore, in contrast with the previous studies, in which a potential effect of the decrease in food intake on obesity and associated disorders has been neglected,[10,15,20] we have attempted to dissect the roles of the decrease in food intake and the effect of CDCA *per se*, respectively, on obesity and energy metabolism by employing pair-feeding strategy. This approach revealed that the reduction of obesity could be mostly explained by the transient decrease in food intake during the initial phase of the intervention, whereas a relatively mild and food intake-independent reduction in adiposity (not detectable at the BW level) could also be observed.

The food intake-independent decrease in adiposity could result from the induction of UCP1-mediated thermogenesis, as suggested by upregulation of the *Ucp1* transcript and the increase in the total UCP1 protein in the interscapular BAT, as well as the upregulation of transcription of selected markers of mitochondrial biogenesis in BAT. This observation is in agreement with the previous study showing TGR5-mediated induction of the *Ucp1* transcript in response to cholic acid.[15] However, to our knowledge, our study demonstrates for the first time an elevation of UCP1 protein content in BAT in response to a BA. This is a critical observation, as UCP1 but not the UCP1 gene transcript is a relevant marker of the BAT thermogenic capacity.[28] The effect of the induction of UCP1-mediated thermogenesis of whole-body energy balance could be substantial for the stabilization of the lean phenotype in the long run, but it could not be detected using indirect calorimetry, reflecting the relatively low sensitivity of this technique and because lean BW data were not available in the present study (see above).

Concerning the inducible UCP1-mediated thermogenesis in brite cells located in WAT (see Introduction), our results document that brite cells could be induced in response to the CDCA intervention. However, in spite of a marked stimulation of the activity of the UCP1 gene at the transcript level observed in scWAT, the amount of UCP1 in the scWAT of the CDCA mice was very low as documented by both, undetectable UCP1 using western blots and a very small fraction of UCP1-positive adipocytes, as revealed using immunohistological analysis. Therefore, induction of UCP1 in interscapular BAT but not in brite cells interspersed in scWAT was probably involved in the induction of EE and lean phenotype in the CDCA mice. It remains to be established whether energy dissipation in other tissues, for example, TGR5-mediated thermogenesis in skeletal muscle,[15] could also be involved.

In spite of the induction of UCP1 in BAT as well the food intake-independent reduction in adiposity in the CDCA mice, indirect calorimetry could not reveal any difference in EE between the CDCA and PF mice, neither when EE per mice nor when EE adjusted to BW was considered. In accordance with the previous studies using cholic acid in cHF-fed mice,[15] also in our study, higher EE adjusted to BW was observed in the CDCA as compared with the cHF mice. However, this effect could be ascribed in full to the inappropriate normalization of EE to BW (see above, and Butler and Kozak[40]), as also documented by equal EE adjusted to BW in the CDCA and the PF mice. In accordance with the previous study using cholic acid,[15] a tendency to decrease RQ in response to the CDCA intervention was observed, which was independent on food intake, and suggested a shift from carbohydrate to lipid oxidation. Nevertheless, RQ changes during the day were affected by the shift in ingestion in the PF group.

Also, changes in gut microbiota can be possibly involved in the effects of CDCA on BAT, because some bacteria can convert CDCA to lithocholic acid, which is a more potent activator of TGR5 (reviewed in Greiner and Backhed [43]). However, this topic was out of the scope of this study.

In conclusion, our results document that CDCA could reduce obesity and associated metabolic disorders in the face of high lipid supply in mice and they suggest a major role of transient reduction in food intake in the anti-obesity effect. Moreover, our results indicate food intake-independent stimulation of UCP1-mediated thermogenesis in BAT in response to CDCA. Although the stimulation of EE in BAT was relatively low and could not be detected using indirect calorimetry, it could be important for the stabilization of the lean phenotype. In addition, the CDCA-induced increase in lipid catabolism could be beneficial with respect to reversal of obesity-associated metabolic disorders. Our results are consistent with the beneficial metabolic effects of BAs, which could be relevant in long-term treatments, but they also warn against overinterpretation of results of some of the previous studies using other BAs.

CONFLICT OF INTEREST

The authors declare no conflict of interest.

ACKNOWLEDGEMENTS

JST, FVD, APG and ATV were recipients of a Fundação para a Ciência e a Tecnologia PhD scholarship (SFRH/BD/38467/2007, SFRH/BD/38372/2007, SFRH/BD/44674/2008 and SFRH/BD/44796/2008, respectively). This project was supported by a FCT grant PTCD/SAU-OSM/72443/2006, PEst-C/SAU/LA0001/2011 and EU FP7 project DIABAT (HEALTH-F2—2011-278373) and by the Czech Science Foundation (13-00871S).

REFERENCES

1 Angelin B, Einarsson K, Hellstrom K, Leijd B. Effects of cholestyramine and chenodeoxycholic acid on the metabolism of endogenous triglyceride in hyperlipoproteinemia. *J Lipid Res* 1978; **19**: 1017–1024.
2 Teodoro JS, Rolo AP, Palmeira CM. Hepatic FXR: key regulator of whole-body energy metabolism. *Trends Endocrinol Metab* 2011; **22**: 458–466.
3 Watanabe M, Houten SM, Wang L, Moschetta A, Mangelsdorf DJ, Heyman RA *et al.* Bile acids lower triglyceride levels via a pathway involving FXR, SHP, and SREBP-1c. *J Clin Invest* 2004; **113**: 1408–1418.
4 Kast HR, Nguyen CM, Sinal CJ, Jones SA, Laffitte BA, Reue K *et al.* Farnesoid X-activated receptor induces apolipoprotein C-II transcription: a molecular mechanism linking plasma triglyceride levels to bile acids. *Mol Endocrinol* 2001; **15**: 1720–1728.
5 Sinal CJ, Tohkin M, Miyata M, Ward JM, Lambert G, Gonzalez FJ. Targeted disruption of the nuclear receptor FXR/BAR impairs bile acid and lipid homeostasis. *Cell* 2000; **102**: 731–744.
6 Stayrook KR, Bramlett KS, Savkur RS, Ficorilli J, Cook T, Christe ME *et al.* Regulation of carbohydrate metabolism by the farnesoid X receptor. *Endocrinology* 2005; **146**: 984–991.
7 Cariou B, van Harmelen K, Duran-Sandoval D, van Dijk TH, Grefhorst A, Abdelkarim M *et al.* The farnesoid X receptor modulates adiposity and peripheral insulin sensitivity in mice. *J Biol Chem* 2006; **281**: 11039–11049.
8 Duran-Sandoval D, Cariou B, Percevault F, Hennuyer N, Grefhorst A, van Dijk TH *et al.* The farnesoid X receptor modulates hepatic carbohydrate metabolism during the fasting-refeeding transition. *J Biol Chem* 2005; **280**: 29971–29979.
9 Abdelkarim M, Caron S, Duhem C, Prawitt J, Dumont J, Lucas A *et al.* The farnesoid X receptor regulates adipocyte differentiation and function by promoting peroxisome proliferator-activated receptor-gamma and interfering with the Wnt/beta-catenin pathways. *J Biol Chem* 2010; **285**: 36759–36767.
10 Watanabe M, Morimoto K, Houten SM, Kaneko-Iwasaki N, Sugizaki T, Horai Y *et al.* Bile acid binding resin improves metabolic control through the induction of energy expenditure. *PloS One* 2012; **7**: e38286.

11 Konikoff FM. Gallstones - approach to medical management. *MedGenMed* 2003; **5**: 8.
12 Prawitt J, Caron S, Staels B. Bile acid metabolism and the pathogenesis of type 2 diabetes. *Curr Diab Rep* 2011; **11**: 160–166.
13 Katona BW, Cummins CL, Ferguson AD, Li T, Schmidt DR, Mangelsdorf DJ *et al.* Synthesis, characterization, and receptor interaction profiles of enantiomeric bile acids. *J Med Chem* 2007; **50**: 6048–6058.
14 Neuschwander-Tetri BA. Farnesoid x receptor agonists: what they are and how they might be used in treating liver disease. *Curr Gastroenterol Rep* 2012; **14**: 55–62.
15 Watanabe M, Houten SM, Mataki C, Christoffolete MA, Kim BW, Sato H *et al.* Bile acids induce energy expenditure by promoting intracellular thyroid hormone activation. *Nature* 2006; **439**: 484–489.
16 Cannon B, Nedergaard J. Brown adipose tissue: function and physiological significance. *Physiol Rev* 2004; **84**: 277–359.
17 Wu J, Cohen P, Spiegelman BM. Adaptive thermogenesis in adipocytes: is beige the new brown? *Genes Dev* 2013; **27**: 234–250.
18 Rothwell NJ, Stock MJ. A role for brown adipose tissue in diet-induced thermogenesis. *Nature* 1979; **281**: 31–35.
19 da-Silva WS, Ribich S, Arrojo e Drigo R, Castillo M, Patti ME, Bianco AC. The chemical chaperones tauroursodeoxycholic and 4-phenylbutyric acid accelerate thyroid hormone activation and energy expenditure. *FEBS Lett* 2011; **585**: 539–544.
20 Watanabe M, Horai Y, Houten SM, Morimoto K, Sugizaki T, Arita E *et al.* Lowering bile acid pool size with a synthetic farnesoid X receptor (FXR) agonist induces obesity and diabetes through reduced energy expenditure. *J Biol Chem* 2011; **286**: 26913–26920.
21 Zingaretti MC, Crosta F, Vitali A, Guerrieri M, Frontini A, Cannon B *et al.* The presence of UCP1 demonstrates that metabolically active adipose tissue in the neck of adult humans truly represents brown adipose tissue. *FASEB J* 2009; **23**: 3113–3120.
22 Young P, Arch JR, Ashwell M. Brown adipose tissue in the parametrial fat pad of the mouse. *FEBS Lett* 1984; **167**: 10–14.
23 Loncar D. Convertible adipose tissue in mice. *Cell Tissue Res* 1991; **266**: 149–161.
24 Cousin B, Cinti S, Morroni M, Raimbault S, Ricquier D, Penicaud L *et al.* Occurrence of brown adipocytes in rat white adipose tissue: molecular and morphological characterization. *J Cell Sci* 1992; **103**: 931–942.
25 Petrovic N, Walden TB, Shabalina IG, Timmons JA, Cannon B, Nedergaard J. Chronic peroxisome proliferator-activated receptor gamma (PPARgamma) activation of epididymally derived white adipocyte cultures reveals a population of thermogenically competent, UCP1-containing adipocytes molecularly distinct from classic brown adipocytes. *J Biol Chem* 2010; **285**: 7153–7164.
26 Frontini A, Vitali A, Perugini J, Murano I, Romiti C, Ricquier D *et al.* White-to-brown transdifferentiation of omental adipocytes in patients affected by pheochromocytoma. *Biochim Biophys Acta* 2013; **1831**: 950–959.
27 Jespersen NZ, Larsen TJ, Peijs L, Daugaard S, Homoe P, Loft A *et al.* A classical brown adipose tissue mRNA signature partly overlaps with brite in the supraclavicular region of adult humans. *Cell Metab* 2013; **17**: 798–805.
28 Nedergaard J, Cannon B. UCP1 mRNA does not produce heat. *Biochim Biophys Acta* 2013; **1831**: 943–949.
29 Kuda O, Jelenik T, Jilkova Z, Flachs P, Rossmeisl M, Hensler M *et al.* n-3 fatty acids and rosiglitazone improve insulin sensitivity through additive stimulatory effects on muscle glycogen synthesis in mice fed a high-fat diet. *Diabetologia* 2009; **52**: 941–951.
30 Medrikova D, Jilkova ZM, Bardova K, Janovska P, Rossmeisl M, Kopecky J. Sex differences during the course of diet-induced obesity in mice: adipose tissue expandability and glycemic control. *Int J Obes* 2012; **36**: 262–272.
31 Rossmeisl M, Jelenik T, Jilkova Z, Slamova K, Kus V, Hensler M *et al.* Prevention and reversal of obesity and glucose intolerance in mice by DHA derivatives. *Obesity* 2009; **17**: 1023–1031.
32 Salmon DM, Flatt JP. Effect of dietary fat content on the incidence of obesity among ad libitum fed mice. *Int J Obes* 1985; **9**: 443–449.
33 Kopecky J, Rossmeisl M, Hodny Z, Syrovy I, Horakova M, Kolarova P. Reduction of dietary obesity in aP2-Ucp transgenic mice: mechanism and adipose tissue morphology. *Am J Physiol* 1996; **270**: E776–E786.
34 Smith PK, Krohn RI, Hermanson GT, Mallia AK, Gartner FH, Provenzano MD *et al.* Measurement of protein using bicinchoninic acid. *Anal Biochem* 1985; **150**: 76–85.
35 Kus V, Prazak T, Brauner P, Hensler M, Kuda O, Flachs P *et al.* Induction of muscle thermogenesis by high-fat diet in mice: association with obesity-resistance. *Am J Physiol Endocrinol Metab* 2008; **295**: E356–E367.
36 Flachs P, Ruhl R, Hensler M, Janovska P, Zouhar P, Kus V *et al.* Synergistic induction of lipid catabolism and anti-inflammatory lipids in white fat of dietary obese mice in response to calorie restriction and n-3 fatty acids. *Diabetologia* 2011; **54**: 2626–2638.
37 Weir JB. New methods for calculating metabolic rate with special reference to protein metabolism. *J Physiol* 1949; **109**: 1–9.
38 Even PC, Nadkarni NA. Indirect calorimetry in laboratory mice and rats: principles, practical considerations, interpretation and perspectives. *Am J Physiol Regul Integr Comp Physiol* 2012; **303**: R459–R476.
39 Seale P, Conroe HM, Estall J, Kajimura S, Frontini A, Ishibashi J *et al.* Prdm16 determines the thermogenic program of subcutaneous white adipose tissue in mice. *J Clin Invest* 2011; **121**: 96–105.
40 Butler AA, Kozak LP. A recurring problem with the analysis of energy expenditure in genetic models expressing lean and obese phenotypes. *Diabetes* 2010; **59**: 323–329.
41 Himms-Hagen J. On raising energy expenditure in ob/ob mice. *Science* 1997; **276**: 1132–1133.
42 Kaiyala KJ, Schwartz MW. Toward a more complete (and less controversial) understanding of energy expenditure and its role in obesity pathogenesis. *Diabetes* 2011; **60**: 17–23.
43 Greiner T, Backhed F. Effects of the gut microbiota on obesity and glucose homeostasis. *Trends Endocrinol Metab* 2011; **22**: 117–123.

Supplementary Information accompanies this paper on International Journal of Obesity website (http://www.nature.com/ijo)